Therapeutic breast reconstruction using gene therapy delivered IFN-gamma immunotherapy

Christopher R. Davis[1,2], Peter A. Than[1], Sacha M.L. Khong[1], Melanie Rodrigues[1], Michael W. Findlay[1,3], Daniel J. Navarrete[1,4], Shadi Ghali[2], Jayant S. Vaidya[2], Geoffrey C. Gurtner[1*]

[1]Stanford University School of Medicine, Stanford University, Stanford, CA, USA

[2]University College London Cancer Institute, University College London, London, UK

[3]Department of Surgery, University of Melbourne, Royal Melbourne Hospital, Parkville, Victoria, Australia

[4]Department of Molecular Biology, Princeton University, Princeton, NJ, USA

*** Corresponding author:** Professor Geoffrey C Gurtner, Stanford University School of Medicine, 257 Campus Drive, GK-201, Stanford University, CA 94305, USA. Email: gcgurtner@stanford.edu; chrisdavis959@hotmail.com

National Presentation: Plastic Surgery Research Council Annual Conference (Seattle, WA, USA)

Submission: *Molecular Cancer Therapeutics*

Figures: 3

Keywords: Gene therapy; Immunotherapy; Autologous; Interferon; Breast cancer

Conflict of interest statement: None

ABSTRACT

After mastectomy, breast reconstruction is increasingly performed using autologous tissue with the aim of improving quality of life. During this procedure, autologous tissue is excised, relocated, and reattached using vascular anastomoses at the site of the extirpated breast. The period during which the tissue is ex vivo may allow genetic modification without any systemic exposure to the vector. Could such access be used to deliver therapeutic agents using the tissue flap as a vehicle? Arguably, such delivery may be more efficient than systemic treatment, in terms of oncological outcomes. The cytokine interferon gamma (IFNγ) has antitumor effects but has severe systemic toxicity that could be circumvented if its effect can be localised by delivery of the IFNγ gene via gene therapy to autologous tissue used for breast reconstruction, which then releases IFNγ and exerts anti-tumor effects. In a rat model of loco-regional recurrence (LRR) with MADB-106-Luc breast cancer cells, autologous tissue was transduced ex vivo with an adeno-associated viral vector (AAV) encoding IFNγ. The therapeutic reconstruction released IFNγ at the LRR site and eliminated cancer cells, significantly decreased tumor burden ($P<0.05$), and increased survival by 33% ($P<0.05$) compared to sham reconstruction. Mechanistically, localized IFNγ immunotherapy stimulated M1 macrophages to target cancer cells within the regional confines of the modified tumor environment. This concept of therapeutic breast reconstruction using ex vivo gene therapy of autologous tissue offers a new application for immunotherapy in breast cancer with a dual therapeutic effect of both reconstructing the ablative defect and delivering local adjuvant immunotherapy.

INTRODUCTION

Breast reconstruction after mastectomy is increasingly performed using autologous tissue to reconstruct the breast after mastectomy,[1] where autologous tissue is frequently moved from the abdomen to the chest to recreate a new breast with the aim of improving quality of life. Over 100,000 cases per annum are performed in the USA,[2] with increasing immediate breast reconstruction clinical practice in the UK and Europe.[3, 4] The procedure involves excising tissue from the patient, and reattaching the autologous tissue at the site of the extirpated breast using microvascular anastomoses. This concept allows access to live tissue ex vivo, and raises the possibility of whether the tissue could be altered during the ex vivo phase, changing it from purely reconstructive tissue to a drug-delivery vehicle of therapeutic agents as a novel adjuvant therapy.

Interferon gamma (IFNγ) is a cytokine with direct and indirect antitumor effects, with oncological mechanisms of activating T cells, macrophages and natural killer (NK) cells towards anti-tumor pathways,[5-8] and targeting tumors via anti-angiogenic pathways, IL-23 inhibition and upregulation of major histocompatibility complex (MHC) I and II cell-surface expression.[9] The therapeutic role of interferon in breast cancer has been reported in a number of recent studies. Firstly, increased IFNγ secondary to emodin stimulation results in attenuation of breast cancer cell growth (4T1 and EO771 breast cancers).[10] Secondly, IFN simulation causes an increase in the anti-cancer efficacy of platinum-based chemotherapy on primary mammary tumors.[11] Thirdly, the tumor microenvironment of triple negative breast cancer is optimized via IFNγ therapy to enable subsequent immune checkpoint blockade therapy.[12] Additionally, IFNγ has a therapeutic role in the wider oncological setting. In pancreatic cancer, direct therapeutic effects of IFNγ are reported, resulting in growth arrest of cancer cells in vitro and maintenance of senescence in vivo.[5] In sarcoma, indirect therapeutic effects of IFNγ have been demonstrated via activation of anti-angiogenesis pathways, resulting in tumor ischemia and cancer cell death.[6] Collectively, these studies support the role of IFNγ as a contemporary therapeutic entity in breast cancer.

The Food and Drug Administration (FDA) approved IFNγ as a treatment modality for osteopetrosis and chronic granulomatous disease (Actimmune, Horizon Pharma PLC, Dublin, Ireland).[13] However, in the oncological setting in a clinical trial of 98 patients, systemically administered IFNγ had an unpredictable response and low efficacy in targeting cancer cells, and resulted in systemic complications in the majority of patients (fever, fatigue, myalgia) due to its diffuse location.[14]

In an attempt to provide high-intensity localized IFNγ therapy for breast cancer, we used gene therapy to deliver the IFNγ gene to autologous tissue that can be used to reconstruct the mastectomy defect. Given the ubiquity of breast reconstructive surgery after mastectomy for breast cancer,[1] the autologous tissue of the reconstructed breast could act as a 'protein pump' releasing IFNγ as a chemotherapeutic agent at the precise anatomical site of future LRRs. This novel vehicle for gene therapy using autologous tissue for therapeutic gain may permit personalized breast cancer therapy that we term 'therapeutic breast reconstruction'. The goal is to reduce LRR and disseminated disease by provide high intensity local therapy, and low systemic therapy, particularly as the LRR can be the harbinger of distant disease.

MATERIALS AND METHODS

Cell Culture

The MADB-106-Luc breast adenocarcinoma cancer cell line (Cell Biolabs, Inc, San Diego, CA) was cultured at 37°C in high glucose Dulbecco's modified Eagle's medium (DMEM), 10% fetal bovine serum (FBS), 0.1 mM MEM Non-Essential Amino Acids (NEAA), 2 mM L-glutamine and 1% penicillin-streptomycin-glutamine (PSG). This cell line was chosen given its malignant properties as a rodent adenocarcinoma, with the luciferase tagging permitting in vivo monitoring of tumor progression. The tipple-negative human breast cancer cell lineage MAD-MB-231-Luc (Sigma-Aldrich, St. Louis, MO, USA) was also used due to the high recurrence rate of tipple-negative breast cancers.

Adipose tissue was harvested [CRD; PT] for in vitro analyses from Female Fischer and RNU rats (Charles River Laboratories, Inc., Wilmington, MA, USA), before physical and collagenase digestion for one hour at 37°C and collagenase inactivation by FBS-supplemented media. Samples were filtered (100µM strainer) and centrifuged. The pellet formed the SVF, which was cultured in DMEM, 10% FBS and 1% PSG (Life Technologies Corporation, Carlsbad, CA, USA) and purified at 37°C in a humidified 5% CO_2 incubator. Cells were used at or before passage three.

Allogeneic macrophages were cultured [CRD; PT] from female Fischer and RNU rat femurs and tibias using a standard protocol for monocytes purification. Stages includes washing samples in sterile media, disaggregating cell clumps, filtration, centrifugation, discarding supernatant, red blood cell lysis, and cell lifting. Macrophage media was DMEM-F12 supplemented with 10% FBS, 1% PSG, and 100U/ml GM-CSF.

Animals

Female Fischer rats (Charles River Laboratories, Inc., Wilmington, MA, USA) were housed in the Stanford University animal facility with food and water ad libitum and circadian light-dark cycling before and after

surgeries. Surgery was conducted [CRD and PT] in the animal operating room using aseptic techniques, post-operative buprinorphine analgesia and 28-day follow-up. Research approval was granted by the Stanford Administrative Panel on Laboratory Animal Care (APLAC #8716) and Biosafety (APB #1431), consistent with the NIH Guide for the Care and Use of Laboratory Animals. Female RNU rats (Charles River Laboratories, Inc., Wilmington, MA, USA) were used for triple-negative breast cancer studies using the MAD-MB-231-Luc cell line, and similar animal welfare practice was followed.

Vector preparation

Viral vectors for treatment (AAV-DJ-CMV-IFNγ) and control (AAV-DJ-CMV-GFP) were produced at the Gene Vector and Virus Core, Stanford School of Medicine, chosen on the basis of its transduction efficiency and the green fluorescent protein (GFP) tagging permitting visualization post transduction. AAV-DJ-CMV-IFNγ was purified (Iodixanol gradient method), produced in T-225 flasks, concentrated (ultrafiltration method) (Fig. S1). Genomic titres were calculated using qPCR and hGH polyA probe and primer, to achieve a copy number of AAV-DJ-CMV-IFNγ at $1.1e^{14}$ vg/ml and AAV-DJ-CMV-GFP at $1.8e^{12}$ vg/ml and later optimized to $1.1e^{14}$ vg/ml. Vector genomes used for in vivo IFN experiments were categorized into high dose ($1.1e^{12}$ vector genomes) and low dose ($1.1e^{11}$ vector genomes). Functional titre (infectious titre) for AAV-DJ-CMV-GFP was quantified at $2.5e^{9}$ IU/ml due to the presence of a reporter gene.

Rat Vascular Endothelial Growth Factor (VEGF) (rVEGF164, Cell Signaling Technology, Danvers, MA, USA) was used with the vector to increase vascular permeability. The formulation was lyophilized from a 0.22 µM filtered solution of phosphate buffered saline (PBS) at pH 7.2, and reconstituted with sterile PBS to a final VEGF concentration of 50 µg/ml. Viles were stored at -20^{o}C, freeze-thaw cycles were minimized and sterility was maintained, before VEGF was solubilized to room temperature for use. The

final vector construct composition included AAV, VEGF, and PBS at 500µL total volume, to match intravascular flap requirements (Fig. 2B). This vector construct was used for all experiments by CD and PT.

Reconstructive Surgery Model

This method is similar to that described previously by our laboratory (Fig. 2A).[15, 16] After isoflurane induction anesthesia, the female Fischer rat was positioned supine with maintenance isoflurane anesthesia. Ventral hair was shaved, and flap dimensions marked over the mammary and adipose tissue. Incision, dissection and flap raise was performed to include the superficial femoral artery and vein supplying and draining the flap. Profunda femoris and the inguinal ligament were preserved. After raising the flap on its blood supply, the autologous tissue was detached from the rodent permitting ex vivo gene therapy (Fig. S2). First, the artery was cannulated and intravascular network of the flap was irrigated with warmed PBS. Second, the vein was clamped using a microvascular clamp. Third, the vector construct was injected via the arterial cannula and the one-hour dwell time commenced. Fourth, the flap was flushed with 3ml PBS to remove excess/unincorporated virions. Fifth, microvascular anastomoses were performed to artery and vein using 10-0 and 11-0 nylon suture (Ethilon, Johnson & Johnson, New Brunswick, NJ, USA) under an operating microscope (Superlux 175, Carl Zeiss, Germany) using microsurgical instruments (S&T AG, Neuhausen, Switzerland). Sixth, to replicate incomplete excision or recurrence, $1x10^6$ MADB-106-Luc breast cancer cells were resuspended in PBS and injected into the tissue plane immediately deep to the flap (Fig. S3). Images were taken using the built-in camera (Universal S3, Carl Zeiss, Germany). Skin incisions were closed with 6-0 nylon suture. Rodents were followed-up for imaging over 28 days, with early termination performed by animal handlers if any uncontrollable signs of distress.

Imaging

Luciferase marking of the MADB-106-Luc and MAD-MB-231-Luc breast cancer cell lines enabled in vitro and in vivo visualization and quantification of light emission using the IVIS™ 100 Imaging System and Living Image 4.4 software (Perkin Elmer, Hopkinton, MA, USA), as outlined by previous methodological data from Stanford,[17] and supported as an independent marker for quantification of luciferase-expressing cells.[18, 19]

After in vivo therapeutic flap experiments, post-operative imaging was performed in a standardized protocol as follows: 15mg/ml luciferin solution was made up by diluting 1g D-Luciferin K Salt with PBS. Luciferin was stored at -20^{o}C and brought to room temperature prior to use. After isoflurane induction and maintenance anaesthesia, the rodent was scanned to establish background emission levels. 5ml luciferin was injected intraperitoneally with an entry point 10mm cranial to the upper flap margin. After waiting 6 minutes, the scan recorded gross values. The region of interest (ROI) box marked over site of cancer cell injection was position in the same place for background and post-injection scans. The background level was subtracted from the gross value to obtain actual emission signal. Dissection microscopy was used to image GFP transduced cells previously transduced by AAV-CMV-GFP under dark room conditions to detect florescence emission.

Fluorescence-activated cell sorting

The potential for the AAV- IFNγ therapeutic flaps to affect the number of local macrophages was examined by comparing macrophage counts (live, CD45+CD68+ cells) within the tissue from the therapeutic flaps (AAV- IFNγ) with control flaps (AAV-GFP) adjacent to the tumor bed 4 weeks after cancer cell injection. Tissue was harvested, mechanically minced using scissors and enzymatically digested (Collagenase A, 0.2U/ml, Roche, Mannheim, Germany) for 1 hour at 37^{o}C before collagenase de-activation with Low Glucose (1g/L D-Glucose) DMEM with L-glutamine, sodium pyruvate (110mg/L) (Life Technologies) and 10% v/v FBS. Following centrifugation (300g, 10minutes), resuspension and 100micron

filtration of the pellet, red cell lysis was performed (Sigma Red Blood Cell Lysing Buffer, 4ml, 5 minutes) at room temperature. Additional DMEM diluted the lysis buffer before re-suspension in fluorescence-activated cell sorting (FACS) buffer (PBS with 2% v/v FBS) for cell counting and FACS antibody labelling. Macrophage-enriched populations (CD45 and CD68 positive live cells) were selected using PE/Cy7 mouse anti-rat CD45 (BD Pharmingen, Clone OX-1) and Alexa Fluor 488 mouse anti-rat CD68 (RioRad) labels. FACS analysis was undertaken following bead-based compensation (BD Comp Bead Plus) on a BD FACS Aria II sorter. Data was analysed using Cytobank 5.0 software with manual gating based on unlabelled, single and double-labelled specimens.

Histological Analysis

Hematoxylin and eosin staining was performed using a standard laboratory protocol by Yugin Park for histological analyses. Dr Richard Luong and Dr. Donna M. Bouley at Stanford Comparative Medicine performed independent analyses of specified tissue samples.

Statistical Analysis

Data were analysed using GraphPad Prism (GraphPad Software Inc., CA, USA). Distribution of data was assessed using Kolmogorov-Smirnov tests. Data were compared between groups using two-tailed unpaired T-tests or Mann-Whitney U tests for parametric and non-parametric data respectively, as well as Chi squared tests for further analyses. Kaplan-Meier survival analyses were performed with post-test Log-rank analyses. Statistical significance was set at $P<0.05$.

RESULTS

Adeno-Associated Viral Vector (AAV) successfully transducts cells in vitro

To demonstrate efficacy of the Adeno-Associated Viral Vector (AAV) constructed for this study, we transduced stromal vascular fraction (SVF) cells in vitro using an AAV with a cytomegalovirus (CMV) promoter producing green fluorescent protein (GFP) (AAV-CMV-GFP) as a control (Fig. 1A). Vector purification, concentration, infectious and genomic titres are outlined in the methods. Allogeneic SVF cells derived from adipose tissue of female rats were used to determine the dosing parameters for the viral vector. AAV-CMV-GFP demonstrated successful in vitro transduction of SVF cells with GFP on fluorescence microscopy analyses (Fig. 1B).

After demonstrating AAV efficacy, AAV-CMV-IFNγ was constructed for the treatment arms of the study (Fig. 1C). After in vitro transduction with AAV-CMV-IFNγ, enzyme-linked immunosorbent assay (ELISA) quantified IFNγ protein release. IFNγ protein release increased incrementally over time in a dose response relationship, with maximum IFNγ protein levels observed after one hour exposure to $1.1e^{12}$ AAV-CMV-IFNγ (Fig. 1D).

Therapeutic flap model successfully releases local protein

Next, in vivo transduction of autologous tissue from female Fischer rats was performed using the AAV-CMV-GFP vector in a therapeutic flap model (Fig. 1E). Autologous tissue was successfully transduced and remained viable for 28 days after the operation, at which point the study ended and the rats were sacrificed. It permitted in vivo natural history analysis of the MADB-106-Luc cancer cell line using AAV-CMV-GFP transduced autologous flaps in female Fischer rat controls. Intravascular flap volume was calculated at 500uL (Fig. 1F), with microvascular anastomosis of superficial femoral artery and vein performed on 1mm diameter vessel lumens (Fig. 1G). To confirm long flap survival and sustained transduction, allogeneic transfer of a luciferase-positive flap into a luciferase-negative host demonstrated

luciferin release on in vivo imaging (Fig. 1H). Successful flap transduction by AAV-CMV-GFP in vivo to autologous tissue was confirmed on fluoroscopic dissection microscopy (Fig. 1I). Thus, this experiment was proof of concept (that transduction was technically possible and tissue remained viable) for a) vector gene-therapy, b) that the vector works. Having proven that a 'therapeutic flap' can be created, we could test whether such a process can be used to deliver a therapeutic agent to the host.

Characterization of the natural history breast cancer cells in control reconstructions (AAV-GFP) and demonstration of effective cancer control after therapeutic flap reconstruction (AAV-IFNγ)

The natural history of MADB-106-Luc breast cancer cells was quantified after control reconstruction. After performing sham reconstructions using the control autologous flap transduced with AAV-CMV-GFP and injecting $1x10^6$ MADB-106-Luc breast cancer cells to the wound base to replicate the clinical scenario of LRR, an increase in luciferase positive breast cancer cells was detected by the in vivo imaging system (IVIS) over time as cancer cells proliferated and the tumor established (Fig. 1J). Histopathological tumor analyses at the site of the control reconstruction identified poorly differentiated cells with atypical morphology and necrosis, consistent with the diagnosis of an established malignant tumor from the MADB-106-Luc breast cancer cells (Figs. 2C and 2D).

Next, we explored in vivo treatment efficacy of rodents undergoing therapeutic reconstruction, where autologous tissue transduced with AAV-CMV-IFNγ was used to reconstruct the defect. The therapeutic flap targeted cancer cell proliferation and increased survival, with in vivo data (n=11) demonstrating a significant decrease in MADB-106-Luc breast cancer cells after therapeutic flap reconstruction with AAV-CMV-IFNγ from day 5 onwards compared to control reconstructions (Two-tailed Mann Whitney U test, P=0.002; Fig. 2A). Rats displayed significantly lower cancer luminescence levels from the flap location site after therapeutic flap reconstruction compared with control flap reconstruction (Fig. 2B and Fig. 2E). After injection of the MADB-106-Luc cancer cells and sham reconstruction, there

was histopathological confirmation of established malignant tumor formation (Fig. 2C and Fig. 2D). Flaps remained viable post-operatively after the experimental sequence of ex vivo AAV transduction, one hour dwell time, saline irrigation, re-anastomosis of blood vessels, and skin suturing, and follow-up (Fig. 2F).

Therapeutic flap in vivo data was similarly efficacious against triple-negative MAD-MB-231-Luc breast cancer cells. Here, a significant decrease in human breast cancer cells was noted after therapeutic flap reconstruction with AAV-CMV-IFNγ compared to sham reconstruction (n=9, Two-tailed Mann Whitney U test, P=0.001; Fig. 2J).

After in vivo studies, tissue from where the tumor cells were injected were surgically excised (by CD) and examined histologically by an independent pathologist (RL). Eradication of the previously injected $1x10^6$ MADB-106-Luc breast cancer cells was noted on independent pathological analysis of the tissue samples, with no evidence of residual neoplastic cells, successful neoplasm suppression, and the presence of scar tissue noted consistent with tumor regression/ destruction (Fig. 2G). Survival advantage from a therapeutic flap reconstruction versus a control reconstruction is shown on the Kaplan-Meier survival plot (Fig. 2H) and the mean survival plot comparing therapeutic flap reconstructions with sham reconstructions (Fig. 2I). Survival increased after therapeutic flap reconstruction, with all included rats in the therapeutic arm surviving to the study end point (day 28) after a single procedure (21 days versus 28 days; unpaired T-test, P=0.04; Log-rank analysis, P=0.18).

Therefore, we demonstrated that interferon gamma (AAV-CMV-IFNγ) delivered locally using a therapeutic flap reduced proliferation of implanted cancer cells of both MADB-106-Luc and MDA-MB-231 cell lineages, with a potential for complete pathological response, and improved overall survival of the animal.

Mechanism of action: therapeutic flap released IFNγ and stimulated macrophages

The IFNγ-producing therapeutic flap resulted in a three-fold increase in macrophages within the surrounding tissues on standard flow analysis (CD45+/CD68+ cells, 21.3% vs 7.4%) when comparing tissue taken in proximity to the control AAV-GFP flap (Fig. 3A) with AAV-IFNγ therapeutic flap (Fig. 3B). These data suggest that the therapeutic flap released IFNγ to stimulate macrophages and exert both direct and indirect downstream anti-tumor effects. In vitro co-culture data further support such a mechanism of macrophage stimulation by IFNγ leading to MADB-106-Luc breast cancer cell death. MADB-106-Luc breast cancer cells in the presence of macrophages and IFNγ demonstrated decreased luminescence and viability (Fig. 3C). Quantitative luminescence data was even more compelling. MADB-106-Luc breast cancer cells co-cultured with macrophages in the absence of IFNγ demonstrated sustained proliferation (and increasing luminescence) whereas those co-cultured with both macrophages and IFNγ showed eradication of cancer cell emission when compared to background (Two-way analysis of variance, $P<0.0001$; Fig. 3D). IFNγ was also demonstrated to exert direct therapeutic effects on breast cancer cells. A significant decrease in cancer cell signal (MAD-MB-231-Luc) after co-culture exposure to IFNγ therapy was quantified (Two-tailed Wilcoxon matched pairs, $P=0.0001$; Fig. 3E). Furthermore, the translational therapeutic goal of the therapeutic flap is to deliver high intensity localized therapy at the exact anatomical location of potential future recurrences, while eliminating any side effects of systemic therapy. Data supporte this, where significantly higher IFNγ protein levels were recorded in the local area after therapeutic flap reconstruction (AAV-CMV-IFNγ) compared to the systemic circulation (unpaired T-test, $P=0.03$; Fig. 3F).

Systemic safety of ex vivo gene therapy and clinical translation towards therapeutic breast reconstruction

With an aim towards clinical trials testing this approach in the patients, we assessed the systemic safety of ex vivo gene therapy. On the analysis of histopathological sections of other systemic tissues remained unchanged in either arm of the study, with no deleterious effect on organ function noted in rodents

undergoing therapeutic flap reconstructions. Specifically, there were no negative consequences to the flap, brain, lung, liver, and kidney in either arm of the study (Fig. 3G).

DISCUSSION

This study demonstrated therapeutic breast reconstruction after breast cancer reduced LRR and increased survival through IFNγ immunotherapy. AAV-CMV-IFNγ successfully transduced autologous tissue with IFNγ, changing it from reconstructive tissue into therapeutic tissue capable of targeting breast cancer cells through a downstream macrophage pathway. This novel immunotherapy approach using ex vivo gene therapy to release IFNγ directly to the tumor bed resulted in a threefold increase in the local macrophage population. Mechanistically, IFNγ exerts direct and indirect oncolytic effects causing growth arrest in cancer cells and macrophage stimulation.[5, 6, 20] In vitro and in vivo data presented suggests IFNγ stimulates monocytes towards a classically activated M1 macrophage lineage,[21] to trigger both adaptive and innate immune systems in a double-pronged attack on cancer cells.[6, 21-24] T-cells may also be involved, in either traditional adaptive pathways or innate-like T cells.[21] This suggestion of both macrophages and T cell involvement is further supported by data exploring therapeutic mechanism of breast cancer cell targeting. After successful therapeutic response of breast cancer to treatment with emodin, an increase in both M1 macrophages and T cells is observed, with a decrease in M2 macrophages.[10]

This mechanism is consistent with proposed therapeutic pathways of IFNγ and macrophages.[5, 6, 24] Macrophage phenotypic plasticity permits controlled direction towards desired functional pathways.[21] IFNγ orchestrates macrophages towards anti-tumor pathways as M1 macrophages,[25] and antagonises tumorogenesis pathways of non-M1 macrophages within the tumor microenvironment of metastasis (TMEM).[26-28] However, identification of the specific type of therapeutic macrophages is challenging due to subtle differences between macrophage subtypes, heterogeneity in cell surface expression, and functional plasticity of cells.[25, 26, 29] Use of IVIS

Macrophage-based therapy has sustained clinical benefits as the half-life varies from hours to years.[30] This has the advantage of targeting residual cancer cells or CSCs to prevent LRR occurring in the five years after mastectomy, which is the exact period when recurrences typically occur.[31] Furthermore, technical obstacles from systemic gene therapy such as imprecise vector specificity, low transgene uptake

and viral limit are overcome using our ex vivo gene therapy approach.[32] Autologous tissue is safely exposed to extremely high viral titres after detachment from the patient, thus overcoming previous limitations, and if there is any indication of harm, the flap can be removed.

One way this approach could be used might be during immediate breast reconstruction after mastectomy for locally advanced breast cancer with a high risk of residual disease despite a large resection. Autologous tissue would normally be harvested from the back or abdomen in current clinical practice for this purpose, and this tissue could be transduced during the ex vivo phase to deliver a therapeutic gene of interest, before anastomosis to chest vessels to complete the therapeutic flap breast reconstruction procedure. In this case, the therapeutic flap would release IFNγ locally at the exact site of the primary tumor to target residual cells or early recurrences, and aim to improve disease-free survival (Fig. 3H). This is especially relevant for clinical translation in oncological cases with a high risk of LRR, such as triple negative breast cancers. Using the therapeutic tissue in these instances as a means of oncological treatment is particularly useful when immediate breast reconstructions are performed, as this early post-operative period of the first five years after diagnosis is the exact time when most LRR diagnoses occur.[31]

Limitations include the following: The LRR model involved injection of cancer cells for subsequent follow-up by IVIS quantification, which may not align with all clinical scenarios of LRR. However, this methodology permitted precise injection of a known cell number for in vivo quantification in a controlled environment that is not possible after tumor establishment and resection models. Furthermore, despite demonstrating local release of the therapeutic protein, protein penetrance was not quantified. However, the mechanism of action of IFNγ is both directly on cancer cells and indirectly on downstream immune upregulation, therefore any cancer cells not in immediate contact with the therapeutic flap would also likely be targeted by the modified TMEM. Other limitations include heterogeneity in cell surface markers for macrophages and their subtypes, phenotypic plasticity, and an unquantified relationship between GFP and luciferin. Future work could quantify the therapeutic response of difference cancer subtypes to the

desired therapeutic protein, in order to inform which patient population would most benefit from therapeutic flap reconstruction. The patients most benefiting from therapeutic flap reconstruction will be those with the most aggressive cancer sub-types and highest rates of LRR despite best current medical and surgical intervention.

Unlike most other breast cancer treatments, breast reconstruction has not been subjected to rigorous large randomized controlled trials to quantify patient benefit or oncological outcomes.[33] Designing such trials has been difficult because of the prevailing belief that patient or surgeon preferences might compromise the equipoise necessary for random allocation. This is an issue,[34] given recent studies[35, 36] suggesting that the trauma and inflammation during delayed breast reconstruction, or soft tissue infections of immediate reconstruction, could stimulate distant metastatic deposits. Given these findings, if breast reconstruction is being performed anyway, any such effects might be counterbalanced if the reconstructed breast is a therapeutic flap that delivers an anti-cancer agent at the same time. A randomized trial to test this hypothesis would then be deemed ethically appropriate.

As further therapeutic proteins and gene mutations are identified, immunotherapy treatment regimens may be tailored to each patient,[37] thus allowing reconstructive tissue to provide an efficacious treatment platform to release desired therapeutic protein to target the primary tumor and prevent recurrent disease in a personalized medicine approach.

CONCLUSION

We successfully constructed and transduced AAV-CMV-IFNγ into cells in vitro and confirmed that it is functionally active by demonstrating an incremental dose-dependent increase in IFNγ protein release. We then demonstrated in vivo flap transduction by AAV-CMV-GFP in vivo to autologous tissue. We successfully created a control model of rat autologous flap reconstruction harboring breast cancer and demonstrated a significant decrease in MADB-106-Luc breast cancer cells after therapeutic flap reconstruction with AAV-CMV-IFNγ from day five onwards compared to control reconstructions, with histopathological evidence of complete eradication of breast cancer. Survival was improved in the therapeutic reconstructed rats compared with controls. A macrophage dependent mechanism was suggested because the IFNγ-producing therapeutic flap resulted in a three-fold increase in macrophages, and breast cancer cells were increasingly targeting when co-cultured with macrophages. These data lead to the possibility of a translational approach applied during immediate breast reconstruction after mastectomy for locally advanced breast cancer in patients with a high risk of residual disease despite a large resection, in order to eliminate the risk of recurrent disease and offer a novel adjuvant therapy with the intention of curing breast cancer after surgical resection.

Figure Legends

Fig. 1. Adeno-Associated Viral Vector (AAV) successfully transduced the stromal vascular fraction (SVF) of adipose tissue with green fluorescent protein (GFP) and interferon gamma (IFNγ) genes, resulting in sustained GFP and IFNγ protein release in a dose response relationship in vitro. Therapeutic flap in vivo control model demonstrated successful AAV transduction of the autologous flap with GFP, resulting in cancer cell proliferation. (**A**) AAV construct of therapeutic flap control with cytomegalovirus (CMV) enhancer and promoter (AAV-DJ-CMV-GFP). (**B**) Fluorescence microscopy images of the SVF of adipose tissue of Fischer rats at Day 1 (left image) and Day 7 (middle image) and RNU rats (right image) after AAV-GFP transduction, with 90% transduction efficiency at Day 7. (**C**) AAV construct of therapeutic flap treatment with CMV promoter (AAV-DJ-CMV-IFNγ). (**D**) Enzyme-linked immunosorbent assay (ELISA) quantification of IFNγ protein release from SVF of adipose tissue after AAV-IFNγ transduction, confirming dose-response relationship after AAV exposure, with increased release of IFNγ protein over time after transduction. (**E**) Experimental therapeutic flap model showing (i) flap harvest; (ii) ex-vivo AAV transduction of flap via artery, before 1 hour dwell time, release of venous clamp, and intravascular irrigation with saline; (iii) microsurgical anastomosis of artery and vein; (iv) injection of MADB-106-Luc breast cancer cells to mimic recurrence; (v) protein release from therapeutic flap reconstruction. (**F**) Ex vivo volume calculation of flap after vascular detachment. (**G**) Microsurgical anastomosis of artery and vein of flap. (**H**) Allogeneic transfer of a luciferase-positive flap into a luciferase-negative host demonstrated sustained flap viability confirmed on in vivo imaging system. (**I**) Successful transduction of flap by AAV-GFP assessed by fluoroscopic dissection microscopy. (**J**) Increase in MADB-106-Luc breast cancer cells after injection and control reconstruction using AAV-GFP flap, with data quantified from light-emitting luciferase positive cancer cells detected by the in vivo imaging system.

Fig. 2. Therapeutic flap transduced with interferon gamma (AAV-IFNγ) significantly decreased cancer cell proliferation and increased survival post therapeutic reconstruction compared to control flap transduced with green fluorescent protein (AAV-GFP). (**A**) Therapeutic flap in vivo data demonstrated significant decrease in MADB-106-Luc breast cancer levels after therapeutic flap reconstruction with AAV-IFNγ from day 5 onwards compared to control. (Mean +/- SEM plotted, two-tailed Mann Whitney U test on non-Gaussian data; n=11; *P<0.05, **P<0.01). (**B**) In vivo image of Fischer rat post AAV-GFP reconstruction (control), demonstrating luminescence from MADB-106-Luc breast cancer cells, where the quantified luminescence emission correlates with the presence of cancer cells. (**C**) Histopathological assessment of tumor tissue confirming the presence of a malignant, poorly differentiated carcinoma with atypical morphology (arrows), consistent with establishment and proliferation of the MADB-106-Luc cells (400X magnification H&E). (**D**) Histopathological assessment of tumor demonstrating solid carcinoma and central necrosis (400X magnification H&E). (**E**) In vivo image of Fischer rat post AAV- IFNγ reconstruction (treatment), demonstrating reduction in cancer cell luminescence. (**F**) Viable therapeutic flap post ex vivo AAV-IFNγ transduction and re-anastomosis. (**G**) Histopathological slide of therapeutic flap tissue (equivalent to Fig. 2F and 2G) at MADB-106-Luc breast cancer injection site, demonstrating no evidence for any residual neoplastic cells, neoplasm successfully suppressed, and scar tissue that develops from a tumor undergoing regression/ destruction. (**H**) Kaplan-Meier survival plot demonstrating survival increase after therapeutic flap reconstruction versus control (Log-rank analysis, P=0.18).(**I**) Survival increased by 33% after therapeutic flap reconstruction compare to control (21 days versus 28 days; unpaired T-test, P=0.04). (**J**) Therapeutic flap in vivo data demonstrated significant decrease in MAD-MB-231-Luc breast cancer levels after therapeutic flap reconstruction with AAV -IFNγ compared to control (Two-tailed Mann Whitney test, n=9; P=0.0012).

Fig. 3. Proposed mechanism of genetically modified therapeutic flap is through local and sustained IFNγ release resulting in IFNγ-mediated stimulation of macrophages to target cancer cells via immunotherapeutic destruction. (**A**) FACS plot of AAV-GFP control flap, demonstrating 7% CD45+/CD68+ cells (macrophages). (**B**) FACS plot of AAV-IFNγ therapeutic flap, demonstrating 21% CD45+/CD68+ cells, suggesting the therapeutic flap releases IFNγ, which stimulates classically activated M1 macrophages, with subsequent downstream anti-cancer effects. (**C**) Co-culture of MADB-106-Luc breast cancer cell line alone as positive control, and after the addition of macrophages, and macrophages plus IFNγ. Luminescence and viability of the cancer cells is eliminated after the addition of macrophages in the presence of IFNγ. (**D**) Quantified bioluminescence data from MADB-106-Luc breast cancer cell emission categorized by co-culture environment over time. Addition of IFNγ to the cancer cell and macrophage co-culture eradicated cancer cell emission. MADB-106-Luc cancer cell emissions increased from day 1 to day 3 in both the cancer group and cancer plus macrophage group, consistent with cancer cell proliferation in the absence of IFNγ (Two-way analysis of variance; $P<0.0001$). (**E**) Cancer cell signal (MAD-MB-231-Luc) significantly decreased after co-culture exposure to IFNγ therapy (Two-tailed Wilcoxon matched pairs, $P=0.0001$). (**F**) Enzyme-linked immunosorbent assay (ELISA) quantification of IFNγ protein release demonstrated significantly higher IFNγ protein levels to the local area after therapeutic flap reconstruction (AAV-CMV-IFNγ) compared to the systemic circulation (1-tail unpaired T-test, $P=0.03$). (**G**) AAV transduced flaps show no gross histologic abnormalities in distant tissue (brain, lung, liver, and kidney), 'Control Tissue' (left column), 'AAV Exposed Tissue' (right column). (**H**) Translational image depicting future clinical application of therapeutic flap in a breast cancer surgical case. A mastectomy is performed and a deep inferior epigastric artery perforator flap is raised from the abdomen (left image), before ex vivo transduction, (center image), and therapeutic flap breast reconstruction with release of the therapeutic protein to target residual cancer cells (right image).

REFERENCES

1. National Mastectomy and Breast Reconstruction Audit. 4th Annual Report. The NHS Information Centre. 2011.
2. Plastic Surgery Statistics Report, 2016. ASPS National Clearinghouse
of Plastic Surgery Procedural Statistics. *American Society of Plastic Surgeons*. Available at:
https://www.plasticsurgery.org/documents/News/Statistics/2016/plastic-surgery-statistics-full-report-2016.pdf.
3. Fancellu A, Sanna V, Cottu P, et al. Mastectomy patterns, but not rates, are changing in the treatment of early breast cancer. Experience of a single European institution on 2315 consecutive patients. *Breast*. 2018;39:1-7.
4. Mennie JC, Mohanna PN, O'Donoghue JM, Rainsbury R, Cromwell DA. National trends in immediate and delayed post-mastectomy reconstruction procedures in England: A seven-year population-based cohort study. *Eur J Surg Oncol*. 2017;43:52-61.
5. Braumuller H, Wieder T, Brenner E, et al. T-helper-1-cell cytokines drive cancer into senescence. *Nature*. 2013;494:361-365.
6. Kammertoens T, Friese C, Arina A, et al. Tumour ischaemia by interferon-gamma resembles physiological blood vessel regression. *Nature*. 2017;545:98-102.
7. Qin Z, Schwartzkopff J, Pradera F, et al. A critical requirement of interferon gamma-mediated angiostasis for tumor rejection by CD8+ T cells. *Cancer Res*. 2003;63:4095-4100.
8. Miller CH, Maher SG, Young HA. Clinical Use of Interferon-gamma. *Ann N Y Acad Sci*. 2009;1182:69-79.
9. Sheikh SZ, Matsuoka K, Kobayashi T, Li F, Rubinas T, Plevy SE. Cutting edge: IFN-gamma is a negative regulator of IL-23 in murine macrophages and experimental colitis. *J Immunol*. 2010;184:4069-4073.
10. Iwanowycz S, Wang J, Hodge J, Wang Y, Yu F, Fan D. Emodin Inhibits Breast Cancer Growth by Blocking the Tumor-Promoting Feedforward Loop between Cancer Cells and Macrophages. *Mol Cancer Ther*. 2016;15:1931-1942.
11. Salvagno C, Ciampricotti M, Tuit S, et al. Therapeutic targeting of macrophages enhances chemotherapy efficacy by unleashing type I interferon response. *Nat Cell Biol*. 2019;21:511-521.
12. Sceneay J, Goreczny GJ, Wilson K, et al. Interferon Signaling is Diminished with Age and is Associated with Immune Checkpoint Blockade Efficacy in Triple-Negative Breast Cancer. *Cancer Discov*. 2019;
13. FDA Approved Drug Products. *The Food and Drug Administration* Available at:
https://www.accessdata.fda.gov/scripts/cder/daf/index.cfm?event=overview.process&applno=103836. Accessed April 19, 2019.
14. Schiller JH, Pugh M, Kirkwood JM, Karp D, Larson M, Borden E. Eastern cooperative group trial of interferon gamma in metastatic melanoma: an innovative study design. *Clin Cancer Res*. 1996;2:29-36.
15. Michaels Jt, Dobryansky M, Galiano RD, et al. Ex vivo transduction of microvascular free flaps for localized peptide delivery. *Ann Plast Surg*. 2004;52:581-584.
16. Michaels Jt, Levine JP, Hazen A, et al. Biologic brachytherapy: ex vivo transduction of microvascular beds for efficient, targeted gene therapy. *Plast Reconstr Surg*. 2006;118:54-65; discussion 66-58.
17. Contag CH, Spilman SD, Contag PR, et al. Visualizing gene expression in living mammals using a bioluminescent reporter. *Photochem Photobiol*. 1997;66:523-531.
18. Tan RP, Lee BSL, Chan AHP, et al. Non-invasive tracking of injected bone marrow mononuclear cells to injury and implanted biomaterials. *Acta Biomater*. 2017;53:378-388.
19. Zanella F, Rosado A, Garcia B, Carnero A, Link W. Using multiplexed regulation of luciferase activity and GFP translocation to screen for FOXO modulators. *BMC Cell Biol*. 2009;10:14.
20. Dighe AS, Richards E, Old LJ, Schreiber RD. Enhanced in vivo growth and resistance to rejection of tumor cells expressing dominant negative IFN gamma receptors. *Immunity*. 1994;1:447-456.
21. Galli SJ, Borregaard N, Wynn TA. Phenotypic and functional plasticity of cells of innate immunity: macrophages, mast cells and neutrophils. *Nat Immunol*. 2011;12:1035-1044.
22. Gordon S, Taylor PR. Monocyte and macrophage heterogeneity. *Nat Rev Immunol*. 2005;5:953-964.
23. Taylor PR, Gordon S. Monocyte heterogeneity and innate immunity. *Immunity*. 2003;19:2-4.
24. Guerriero JL, Sotayo A, Ponichtera HE, et al. Class IIa HDAC inhibition reduces breast tumours and metastases through anti-tumour macrophages. *Nature*. 2017;543:428-432.
25. Biswas SK, Mantovani A. Macrophage plasticity and interaction with lymphocyte subsets: cancer as a paradigm. *Nat Immunol*. 2010;11:889-896.
26. Mosser DM, Edwards JP. Exploring the full spectrum of macrophage activation. *Nat Rev Immunol*. 2008;8:958-969.

27. Nardin A, Abastado JP. Macrophages and cancer. *Front Biosci*. 2008;13:3494-3505.
28. Pollard JW. Tumour-educated macrophages promote tumour progression and metastasis. *Nat Rev Cancer*. 2004;4:71-78.
29. Ambarus CA, Krausz S, van Eijk M, et al. Systematic validation of specific phenotypic markers for in vitro polarized human macrophages. *J Immunol Methods*. 2012;375:196-206.
30. Geissmann F, Manz MG, Jung S, Sieweke MH, Merad M, Ley K. Development of monocytes, macrophages, and dendritic cells. *Science*. 2010;327:656-661.
31. Li Y, Rosen JM. Stem/progenitor cells in mouse mammary gland development and breast cancer. *J Mammary Gland Biol Neoplasia*. 2005;10:17-24.
32. Mingozzi F, Anguela XM, Pavani G, et al. Overcoming preexisting humoral immunity to AAV using capsid decoys. *Sci Transl Med*. 2013;5:194ra192.
33. D'Souza N, Darmanin G, Fedorowicz Z. Immediate versus delayed reconstruction following surgery for breast cancer. *Cochrane Database Syst Rev*. 2011;Cd008674.
34. Vaidya J. *Perioperative Inflammation as Triggering Origin of Metastasis Development*: in The Systemic Effects of Local Treatments (Surgery and Radiotherapy) of Breast Cancer. Published by Springer International Publishing AG. Editors MW Retsky, R Demicheli; 2017.
35. Beecher SM, O'Leary DP, McLaughlin R, Sweeney KJ, Kerin MJ. Influence of complications following immediate breast reconstruction on breast cancer recurrence rates. *Br J Surg*. 2016;103:391-398.
36. Dillekas H, Demicheli R, Ardoino I, Jensen SAH, Biganzoli E, Straume O. The recurrence pattern following delayed breast reconstruction after mastectomy for breast cancer suggests a systemic effect of surgery on occult dormant micrometastases. *Breast Cancer Res Treat*. 2016;158:169-178.
37. Patel SJ, Sanjana NE, Kishton RJ, et al. Identification of essential genes for cancer immunotherapy. *Nature*. 2017;548:537-542.

Funding: National Institutes of Health (RO1 - EB005718-01A1), the Armed Forces Institute of Regenerative Medicine, the Hagey Family Endowed Fund in Stem Cell Research and Regenerative Medicine, the American College of Surgeons, the Royal College of Surgeons of England, the US-UK Fulbright Commission

Ethics committee approval: Research approval was granted by the Stanford Administrative Panel on Laboratory Animal Care (APLAC #8716) and Biosafety (APB #1431), consistent with the NIH Guide for the Care and Use of Laboratory Animals.

Fig. 1

A

B

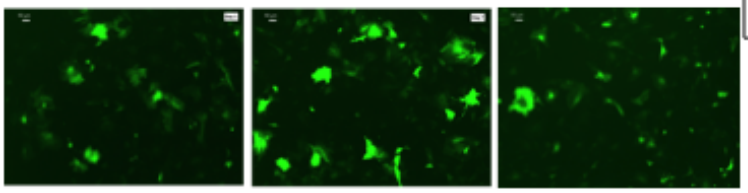

C

D

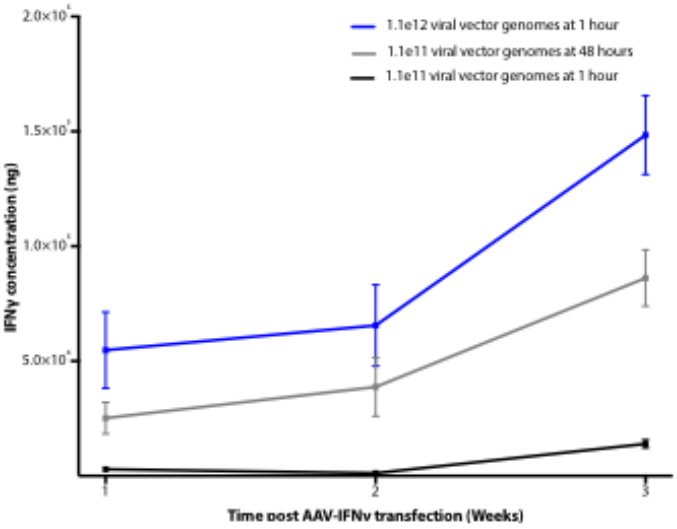

E

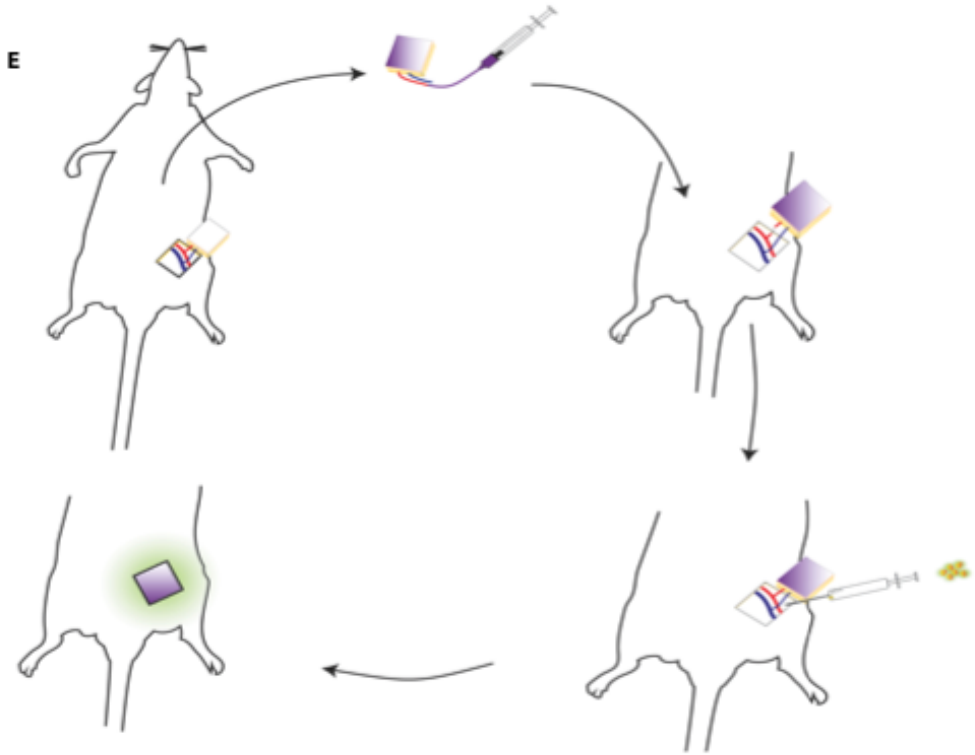

F

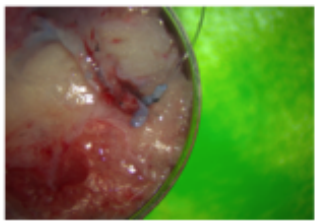

G

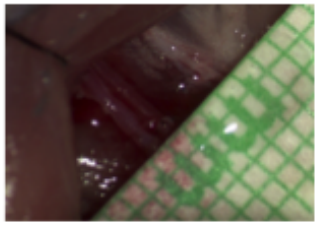

H

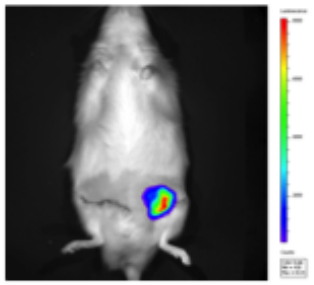

I

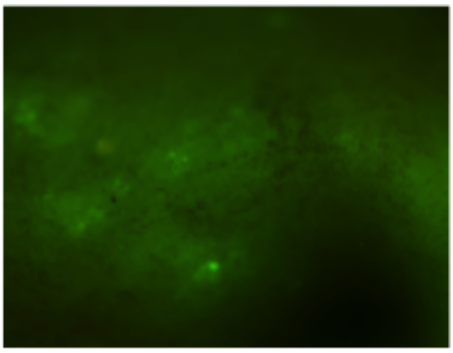

J

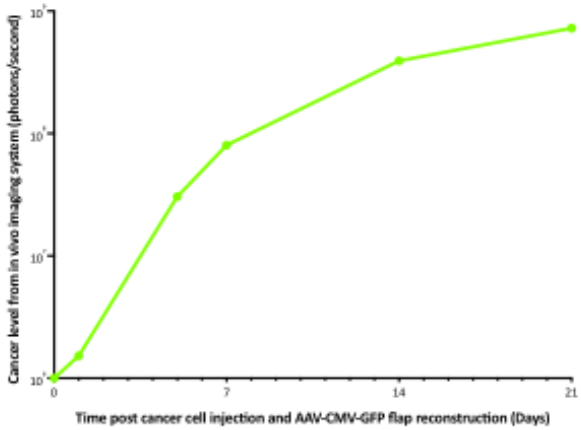

Fig. 2

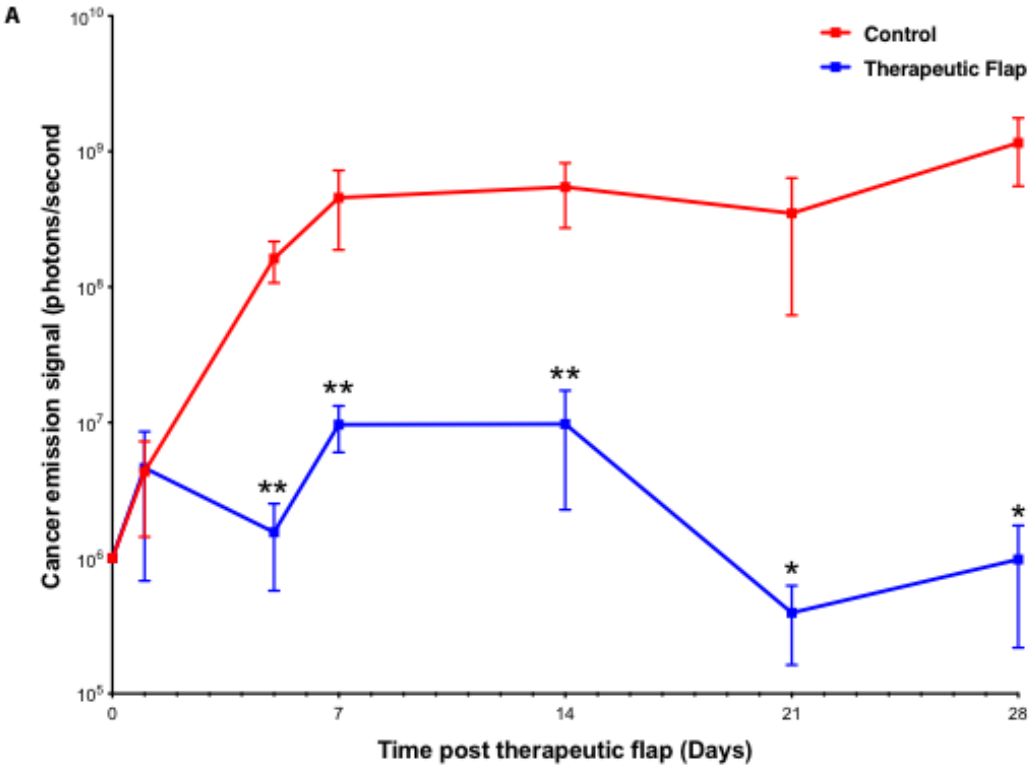
A
Control
Therapeutic Flap
Cancer emission signal (photons/second
Time post therapeutic flap (Days)
**
**
**
*
*

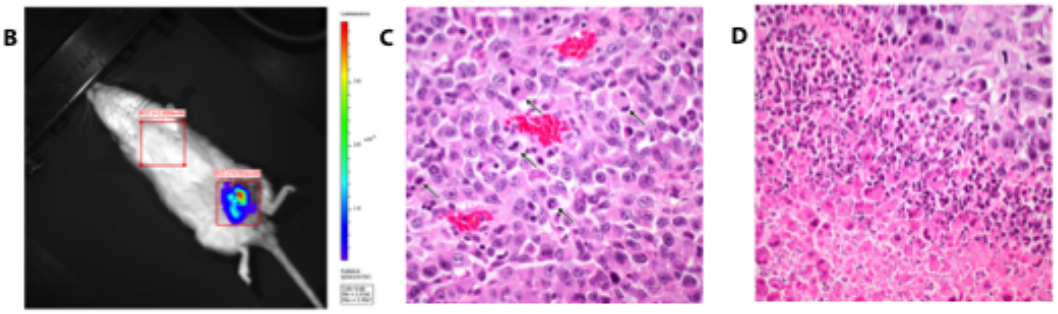
B
C
D

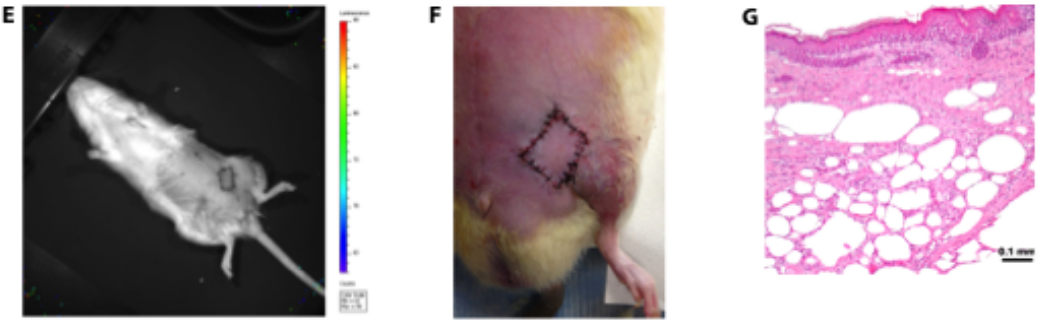
E
F
G

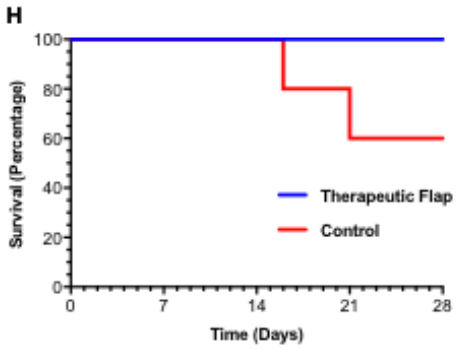
H
Survival (Percentage)
Therapeutic Flap
Control
Time (Days)

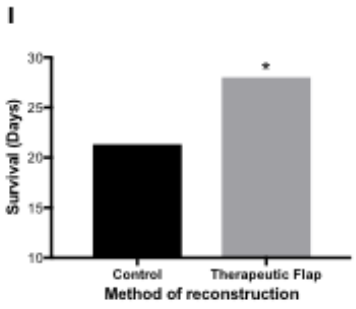
I
Survival (Days)
*
Control
Therapeutic Flap
Method of reconstruction

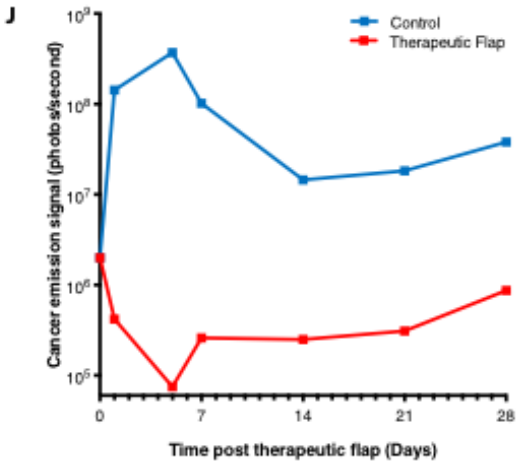
J
Control
Therapeutic Flap
Cancer emission signal (photons/second)
Time post therapeutic flap (Days)

Fig. 3

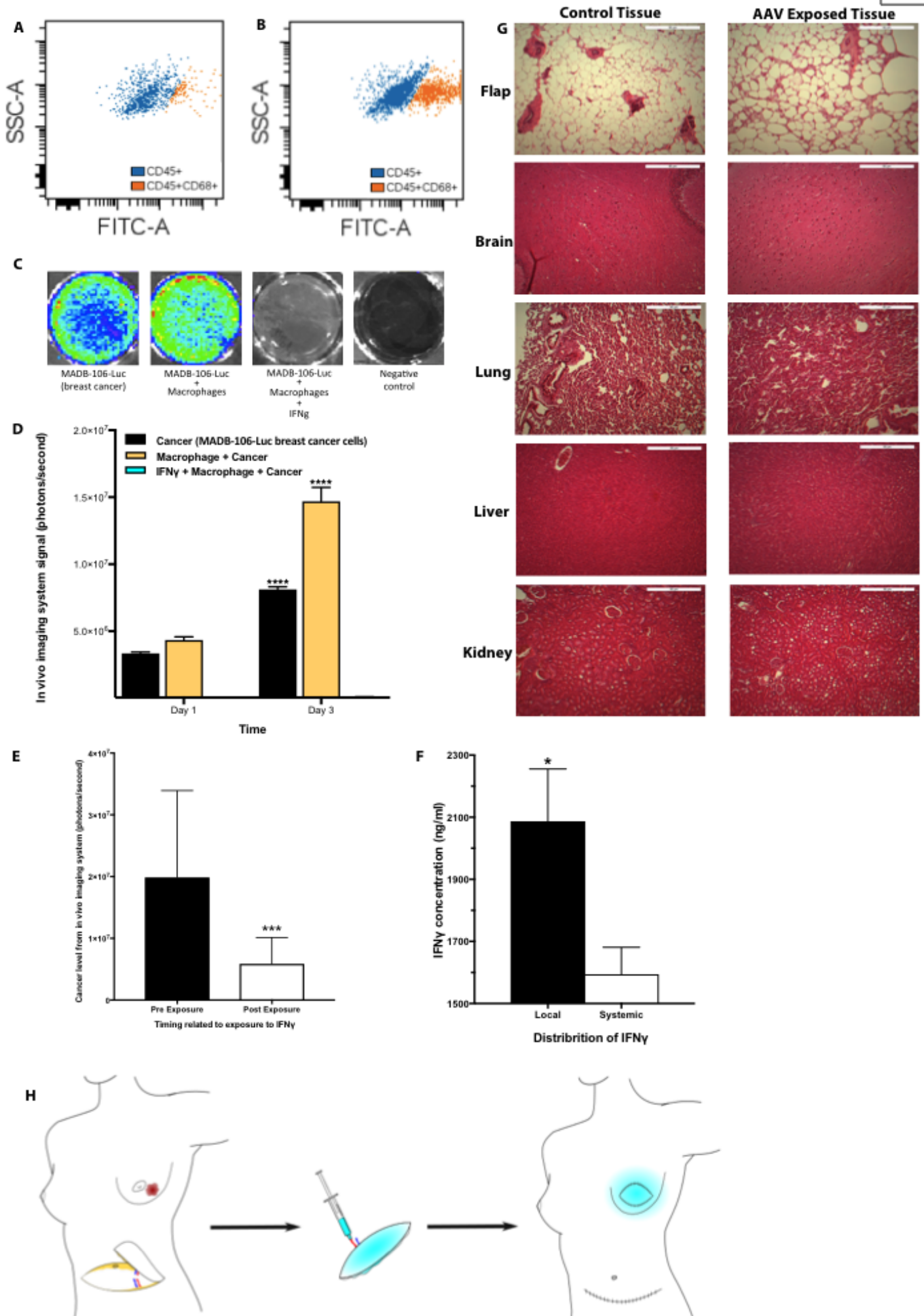
A
SSC-A
FITC-A
CD45+
CD45+CD68+
B
SSC-A
FITC-A
CD45+
CD45+CD68+
C
MADB-106-Luc (breast cancer)
MADB-106-Luc + Macrophages
MADB-106-Luc + Macrophages + IFNg
Negative control
D
In vivo imaging system signal (photons/second)
Cancer (MADB-106-Luc breast cancer cells)
Macrophage + Cancer
IFNγ + Macrophage + Cancer
Day 1
Day 3
Time
E
Cancer level from in vivo imaging system (photons/second)
Pre Exposure
Post Exposure
Timing related to exposure to IFNγ
F
IFNγ concentration (ng/ml)
Local
Systemic
Distribrition of IFNγ
G
Control Tissue
AAV Exposed Tissue
Flap
Brain
Lung
Liver
Kidney
H